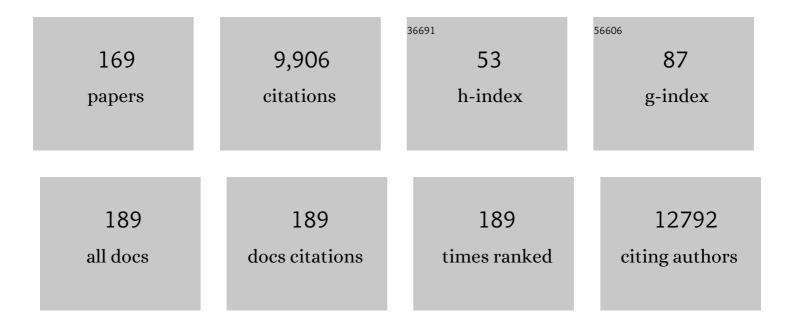
List of Publications by Year in descending order

Source: https://exaly.com/author-pdf/6402350/publications.pdf Version: 2024-02-01



#	Article	IF	CITATIONS
1	Multiple conformations of trimeric spikes visualized on a non-enveloped virus. Nature Communications, 2022, 13, 550.	5.8	6
2	Structural basis of RNA conformational switching in the transcriptional regulator 7SK RNP. Molecular Cell, 2022, 82, 1724-1736.e7.	4.5	18
3	Structure of active human telomerase with telomere shelterin protein TPP1. Nature, 2022, 604, 578-583.	13.7	43
4	Locations and in situ structure of the polymerase complex inside the virion of vesicular stomatitis virus. Proceedings of the National Academy of Sciences of the United States of America, 2022, 119, e2111948119.	3.3	6
5	Structure, dynamics and assembly of the ankyrin complex on human red blood cell membrane. Nature Structural and Molecular Biology, 2022, 29, 698-705.	3.6	18
6	Structure of Tetrahymena telomerase-bound CST with polymerase \hat{I}_{\pm} -primase. Nature, 2022, 608, 813-818.	13.7	29
7	Cryo-EM structures reveal the molecular basis of receptor-initiated coxsackievirus uncoating. Cell Host and Microbe, 2021, 29, 448-462.e5.	5.1	19
8	Protein identification from electron cryomicroscopy maps by automated model building and side-chain matching. Acta Crystallographica Section D: Structural Biology, 2021, 77, 457-462.	1.1	9
9	Atomic Structure of the Trichomonas vaginalis Double-Stranded RNA Virus 2. MBio, 2021, 12, .	1.8	6
10	Structures of telomerase at several steps of telomere repeat synthesis. Nature, 2021, 593, 454-459.	13.7	44
11	Asymmetric reconstruction of mammalian reovirus reveals interactions among RNA, transcriptional factor µ2 and capsid proteins. Nature Communications, 2021, 12, 4176.	5.8	20
12	Encapsulation state of messenger RNA inside lipid nanoparticles. Biophysical Journal, 2021, 120, 2766-2770.	0.2	86
13	Structure of the trypanosome paraflagellar rod and insights into non-planar motility of eukaryotic cells. Cell Discovery, 2021, 7, 51.	3.1	12
14	Identification and architecture of a putative secretion tube across mycobacterial outer envelope. Science Advances, 2021, 7, .	4.7	2
15	Native structure of the RhopH complex, a key determinant of malaria parasite nutrient acquisition. Proceedings of the National Academy of Sciences of the United States of America, 2021, 118, .	3.3	20
16	Structure of human cytomegalovirus virion reveals host tRNA binding to capsid-associated tegument protein pp150. Nature Communications, 2021, 12, 5513.	5.8	13
17	Cryo-EM structure of the sodium-driven chloride/bicarbonate exchanger NDCBE. Nature Communications, 2021, 12, 5690.	5.8	24
18	Cross-neutralizing antibodies bind a SARS-CoV-2 cryptic site and resist circulating variants. Nature Communications, 2021, 12, 5652.	5.8	49

#	Article	IF	CITATIONS
19	Bluetongue virus capsid protein VP5 perforates membranes at low endosomal pH during viral entry. Nature Microbiology, 2021, 6, 1424-1432.	5.9	14
20	The epitope arrangement on flavivirus particles contributes to Mab C10's extraordinary neutralization breadth across Zika and dengue viruses. Cell, 2021, 184, 6052-6066.e18.	13.5	38
21	Bottom-up structural proteomics: cryoEM of protein complexes enriched from the cellular milieu. Nature Methods, 2020, 17, 79-85.	9.0	80
22	Atomic Structures of Anthrax Prechannel Bound with Full-Length Lethal and Edema Factors. Structure, 2020, 28, 879-887.e3.	1.6	8
23	Structural basis for STAT2 suppression by flavivirus NS5. Nature Structural and Molecular Biology, 2020, 27, 875-885.	3.6	40
24	A Calcium Sensor Discovered in Bluetongue Virus Nonstructural Protein 2 Is Critical for Virus Replication. Journal of Virology, 2020, 94, .	1.5	10
25	Structural Basis for Capsid Recruitment and Coat Formation during HSV-1 Nuclear Egress. Proceedings (mdpi), 2020, 50, 101.	0.2	0
26	Structures of capsid and capsid-associated tegument complex inside the Epstein–Barr virus. Nature Microbiology, 2020, 5, 1285-1298.	5.9	14
27	D-loop Dynamics and Near-Atomic-Resolution Cryo-EM Structure of Phalloidin-Bound F-Actin. Structure, 2020, 28, 586-593.e3.	1.6	26
28	Mesophasic organization of GABAA receptors in hippocampal inhibitory synapses. Nature Neuroscience, 2020, 23, 1589-1596.	7.1	52
29	Near-atomic cryo-electron microscopy structures of varicella-zoster virus capsids. Nature Microbiology, 2020, 5, 1542-1552.	5.9	7
30	Genome organization and interaction with capsid protein in a multipartite RNA virus. Proceedings of the United States of America, 2020, 117, 10673-10680.	3.3	31
31	Lexis and Grammar of Mitochondrial RNA Processing in Trypanosomes. Trends in Parasitology, 2020, 36, 337-355.	1.5	71
32	Biphasic exocytosis of herpesvirus from hippocampal neurons and mechanistic implication to membrane fusion. Cell Discovery, 2020, 6, 2.	3.1	6
33	Identification of Antibodies with Non-overlapping Neutralization Sites that Target Coxsackievirus A16. Cell Host and Microbe, 2020, 27, 249-261.e5.	5.1	24
34	Architecture of the herpesvirus genome-packaging complex and implications for DNA translocation. Protein and Cell, 2020, 11, 339-351.	4.8	53
35	Action of a minimal contractile bactericidal nanomachine. Nature, 2020, 580, 658-662.	13.7	61
36	Atomic structures of anthrax toxin protective antigen channels bound to partially unfolded lethal and edema factors. Nature Communications, 2020, 11, 840.	5.8	28

#	Article	IF	CITATIONS
37	Structural basis for capsid recruitment and coat formation during HSV-1 nuclear egress. ELife, 2020, 9, .	2.8	30
38	In situ structures of RNA-dependent RNA polymerase inside bluetongue virus before and after uncoating. Proceedings of the National Academy of Sciences of the United States of America, 2019, 116, 16535-16540.	3.3	34
39	An efficient protocol of cryo-correlative light and electron microscopy for the study of neuronal synapses. Biophysics Reports, 2019, 5, 111-122.	0.2	12
40	Atomic Structure of the Francisella T6SS Central Spike Reveals a Unique α-Helical Lid and a Putative Cargo. Structure, 2019, 27, 1811-1819.e6.	1.6	6
41	Conservative transcription in three steps visualized in a double-stranded RNA virus. Nature Structural and Molecular Biology, 2019, 26, 1023-1034.	3.6	33
42	DNA-Packing Portal and Capsid-Associated Tegument Complexes in the Tumor Herpesvirus KSHV. Cell, 2019, 178, 1329-1343.e12.	13.5	45
43	A unified mechanism for intron and exon definition and back-splicing. Nature, 2019, 573, 375-380.	13.7	114
44	CryoEM structures of Arabidopsis DDR complexes involved in RNA-directed DNA methylation. Nature Communications, 2019, 10, 3916.	5.8	31
45	Structures and operating principles of the replisome. Science, 2019, 363, .	6.0	119
46	Cryo-EM structures of herpes simplex virus type 1 portal vertex and packaged genome. Nature, 2019, 570, 257-261.	13.7	111
47	In situ structures of rotavirus polymerase in action and mechanism of mRNA transcription and release. Nature Communications, 2019, 10, 2216.	5.8	65
48	Structure of the human ClC-1 chloride channel. PLoS Biology, 2019, 17, e3000218.	2.6	66
49	pH-dependent gating mechanism of the <i>Helicobacter pylori</i> urea channel revealed by cryo-EM. Science Advances, 2019, 5, eaav8423.	4.7	20
50	Postsynaptic protein organization revealed by electron microscopy. Current Opinion in Structural Biology, 2019, 54, 152-160.	2.6	27
51	Atomic structure of the translation regulatory protein NS1 of bluetongue virus. Nature Microbiology, 2019, 4, 837-845.	5.9	23
52	Atomic structures and deletion mutant reveal different capsid-binding patterns and functional significance of tegument protein pp150 in murine and human cytomegaloviruses with implications for therapeutic development. PLoS Pathogens, 2019, 15, e1007615.	2.1	13
53	Atomic structure of the human herpesvirus 6B capsid and capsid-associated tegument complexes. Nature Communications, 2019, 10, 5346.	5.8	16
54	Cryo electron tomography with volta phase plate reveals novel structural foundations of the 96-nm axonemal repeat in the pathogen Trypanosoma brucei. ELife, 2019, 8, .	2.8	46

#	Article	IF	CITATIONS
55	Electron Cryo-microscopy Structure of Ebola Virus Nucleoprotein Reveals a Mechanism for Nucleocapsid-like Assembly. Cell, 2018, 172, 966-978.e12.	13.5	51
56	CryoEM structure of the human SLC4A4 sodium-coupled acid-base transporter NBCe1. Nature Communications, 2018, 9, 900.	5.8	78
57	Atomic Structure of the E2 Inner Core of Human Pyruvate Dehydrogenase Complex. Biochemistry, 2018, 57, 2325-2334.	1.2	28
58	Structure of the herpes simplex virus 1 capsid with associated tegument protein complexes. Science, 2018, 360, .	6.0	133
59	Molecular basis for CENP-N recognition of CENP-A nucleosome on the human kinetochore. Cell Research, 2018, 28, 374-378.	5.7	65
60	Structure and mutagenesis reveal essential capsid protein interactions for KSHV replication. Nature, 2018, 553, 521-525.	13.7	44
61	Structural basis of TRPV5 channel inhibition by econazole revealed by cryo-EM. Nature Structural and Molecular Biology, 2018, 25, 53-60.	3.6	114
62	Membrane insertion of—and membrane potential sensing by—semiconductor voltage nanosensors: Feasibility demonstration. Science Advances, 2018, 4, e1601453.	4.7	33
63	Differentiation and Characterization of Excitatory and Inhibitory Synapses by Cryo-electron Tomography and Correlative Microscopy. Journal of Neuroscience, 2018, 38, 1493-1510.	1.7	136
64	Solution Structures of Engineered Vault Particles. Structure, 2018, 26, 619-626.e3.	1.6	14
65	Atomic-level evidence for packing and positional amyloid polymorphism by segment from TDP-43 RRM2. Nature Structural and Molecular Biology, 2018, 25, 311-319.	3.6	89
66	Different functional states of fusion protein gB revealed on human cytomegalovirus by cryo electron tomography with Volta phase plate. PLoS Pathogens, 2018, 14, e1007452.	2.1	80
67	Discovery and structural characterization of a therapeutic antibody against coxsackievirus A10. Science Advances, 2018, 4, eaat7459.	4.7	19
68	De novo computational RNA modeling into cryo-EM maps of large ribonucleoprotein complexes. Nature Methods, 2018, 15, 947-954.	9.0	45
69	Cryo-EM of full-length α-synuclein reveals fibril polymorphs with a common structural kernel. Nature Communications, 2018, 9, 3609.	5.8	468
70	Structure of Telomerase with Telomeric DNA. Cell, 2018, 173, 1179-1190.e13.	13.5	124
71	<i>In Situ</i> Structures of the Polymerase Complex and RNA Genome Show How Aquareovirus Transcription Machineries Respond to Uncoating. Journal of Virology, 2018, 92, .	1.5	28
72	Accumulation of Dense Core Vesicles in Hippocampal Synapses Following Chronic Inactivity. Frontiers in Neuroanatomy, 2018, 12, 48.	0.9	20

#	Article	IF	CITATIONS
73	Cryo-EM structure of the human $\hat{1}\pm5\hat{1}^2$ 3 GABAA receptor. Cell Research, 2018, 28, 958-961.	5.7	21
74	Malaria parasite translocon structure and mechanism of effector export. Nature, 2018, 561, 70-75.	13.7	169
75	Building atomic models based on near atomic resolution cryoEM maps with existing tools. Journal of Structural Biology, 2018, 204, 313-318.	1.3	14
76	Polypeptide-Based Gold Nanoshells for Photothermal Therapy. SLAS Technology, 2017, 22, 18-25.	1.0	13
77	CryoEM structure of the Methanospirillum hungatei archaellum reveals structural features distinct from the bacterial flagellum and type IV pilus. Nature Microbiology, 2017, 2, 16222.	5.9	72
78	In situ structures of the genome and genome-delivery apparatus in a single-stranded RNA virus. Nature, 2017, 541, 112-116.	13.7	137
79	Conformation-Directed Formation of Self-Healing Diblock Copolypeptide Hydrogels via Polyion Complexation. Journal of the American Chemical Society, 2017, 139, 15114-15121.	6.6	72
80	Monomeric ephrinB2 binding induces allosteric changes in Nipah virus G that precede its full activation. Nature Communications, 2017, 8, 781.	5.8	38
81	Atomic Structures of Minor Proteins VI and VII in Human Adenovirus. Journal of Virology, 2017, 91, .	1.5	59
82	Inhibition of EBV-mediated membrane fusion by anti-gHgL antibodies. Proceedings of the National Academy of Sciences of the United States of America, 2017, 114, E8703-E8710.	3.3	27
83	Atomic structures of Coxsackievirus A6 and its complex with a neutralizing antibody. Nature Communications, 2017, 8, 505.	5.8	61
84	Structure of the yeast spliceosomal postcatalytic P complex. Science, 2017, 358, 1278-1283.	6.0	87
85	Atomic structure of the human cytomegalovirus capsid with its securing tegument layer of pp150. Science, 2017, 356, .	6.0	94
86	Engineering A11 Minibody-Conjugated, Polypeptide-Based Gold Nanoshells for Prostate Stem Cell Antigen (PSCA)–Targeted Photothermal Therapy. SLAS Technology, 2017, 22, 26-35.	1.0	11
87	A pUL25 dimer interfaces the pseudorabies virus capsid and tegument. Journal of General Virology, 2017, 98, 2837-2849.	1.3	27
88	Discovery and Characterization of Iron Sulfide and Polyphosphate Bodies Coexisting in <i>Archaeoglobus fulgidus</i> Cells. Archaea, 2016, 2016, 1-11.	2.3	45
89	In situ Structure of Viral RNA by Cryo Electron Tomography with Volta Phase Plate, Energy Filtering and Direct Electron Counting. Microscopy and Microanalysis, 2016, 22, 74-75.	0.2	1
90	Structure of the Full-Length TRPV2 Channel by Cryo-EM. Microscopy and Microanalysis, 2016, 22, 1118-1119.	0.2	0

#	Article	IF	CITATIONS
91	Structure and Conductivity of Semiconducting Polymer Hydrogels. Journal of Physical Chemistry B, 2016, 120, 6215-6224.	1.2	14
92	F-Type Bacteriocins of Listeria monocytogenes: a New Class of Phage Tail-Like Structures Reveals Broad Parallel Coevolution between Tailed Bacteriophages and High-Molecular-Weight Bacteriocins. Journal of Bacteriology, 2016, 198, 2784-2793.	1.0	41
93	Structure of the full-length TRPV2 channel by cryo-EM. Nature Communications, 2016, 7, 11130.	5.8	176
94	Structures and stabilization of kinetoplastid-specific split rRNAs revealed by comparing leishmanial and human ribosomes. Nature Communications, 2016, 7, 13223.	5.8	48
95	Complete genome sequence of Methanospirillum hungatei type strain JF1. Standards in Genomic Sciences, 2016, 11, 2.	1.5	33
96	Atomic model of a nonenveloped virus reveals pH sensors for a coordinated process of cell entry. Nature Structural and Molecular Biology, 2016, 23, 74-80.	3.6	50
97	Phenotypic and Physiological Characterization of the Epibiotic Interaction Between TM7x and Its Basibiont Actinomyces. Microbial Ecology, 2016, 71, 243-255.	1.4	68
98	Conserved SMP domains of the ERMES complex bind phospholipids and mediate tether assembly. Proceedings of the National Academy of Sciences of the United States of America, 2015, 112, E3179-88.	3.3	174
99	CryoEM and mutagenesis reveal that the smallest capsid protein cements and stabilizes Kaposi's sarcoma-associated herpesvirus capsid. Proceedings of the National Academy of Sciences of the United States of America, 2015, 112, E649-56.	3.3	27
100	Atomic Structure of T6SS Reveals Interlaced Array Essential to Function. Cell, 2015, 160, 940-951.	13.5	155
101	Long-lived photoinduced polaron formation in conjugated polyelectrolyte-fullerene assemblies. Science, 2015, 348, 1340-1343.	6.0	53
102	Atomic structure of anthrax protective antigen pore elucidates toxin translocation. Nature, 2015, 521, 545-549.	13.7	217
103	Atomic structures of a bactericidal contractile nanotube in its pre- and postcontraction states. Nature Structural and Molecular Biology, 2015, 22, 377-382.	3.6	134
104	In situ structures of the segmented genome and RNA polymerase complex inside a dsRNA virus. Nature, 2015, 527, 531-534.	13.7	93
105	Structure of <i>Tetrahymena</i> telomerase reveals previously unknown subunits, functions, and interactions. Science, 2015, 350, aab4070.	6.0	134
106	Three-dimensional organization of nascent rod outer segment disk membranes. Proceedings of the National Academy of Sciences of the United States of America, 2015, 112, 14870-14875.	3.3	73
107	A new class of highly potent, broadly neutralizing antibodies isolated from viremic patients infected with dengue virus. Nature Immunology, 2015, 16, 170-177.	7.0	415
108	Crystal Structure of the Pre-fusion Nipah Virus Fusion Glycoprotein Reveals a Novel Hexamer-of-Trimers Assembly. PLoS Pathogens, 2015, 11, e1005322.	2.1	59

#	Article	IF	CITATIONS
109	Protein chainmail variants in dsDNA viruses. AIMS Biophysics, 2015, 2, 200-218.	0.3	9
110	A putative ATPase mediates RNA transcription and capping in a dsRNA virus. ELife, 2015, 4, e07901.	2.8	33
111	Cumulative effects of the ApoE genotype and gender on the synaptic proteome and oxidative stress in the mouse brain. International Journal of Neuropsychopharmacology, 2014, 17, 1863-1879.	1.0	28
112	Assembly and Architecture of the EBV B Cell Entry Triggering Complex. PLoS Pathogens, 2014, 10, e1004309.	2.1	68
113	Cryo-EM reveals different coronin binding modes for ADP– and ADP–BeFx actin filaments. Nature Structural and Molecular Biology, 2014, 21, 1075-1081.	3.6	45
114	Association of Herpes Simplex Virus pU _L 31 with Capsid Vertices and Components of the Capsid Vertex-Specific Complex. Journal of Virology, 2014, 88, 3815-3825.	1.5	46
115	Single particle analysis integrated with microscopy: A high-throughput approach for reconstructing icosahedral particles. Journal of Structural Biology, 2014, 186, 8-18.	1.3	4
116	Structures of viral membrane proteins by high-resolution cryoEM. Current Opinion in Virology, 2014, 5, 111-119.	2.6	8
117	Chaperone fusion proteins aid entropy-driven maturation of class II viral fusion proteins. Trends in Microbiology, 2014, 22, 100-106.	3.5	8
118	Organization of Capsid-Associated Tegument Components in Kaposi's Sarcoma-Associated Herpesvirus. Journal of Virology, 2014, 88, 12694-12702.	1.5	49
119	Four Levels of Hierarchical Organization, Including Noncovalent Chainmail, Brace the Mature Tumor Herpesvirus Capsid against Pressurization. Structure, 2014, 22, 1385-1398.	1.6	16
120	INF2-Mediated Severing through Actin Filament Encirclement and Disruption. Current Biology, 2014, 24, 156-164.	1.8	48
121	IRE1 Phosphatase PP2Ce Regulates Adaptive ER Stress Response in the Postpartum Mammary Gland. PLoS ONE, 2014, 9, e111606.	1.1	17
122	Purification of Herpesvirus Virions and Capsids. Bio-protocol, 2014, 4, .	0.2	12
123	<i>Tetrahymena</i> Telomerase Holoenzyme Assembly, Activation, and Inhibition by Domains of the p50 Central Hub. Molecular and Cellular Biology, 2013, 33, 3962-3971.	1.1	25
124	Protein interactions in the murine cytomegalovirus capsid revealed by cryoEM. Protein and Cell, 2013, 4, 833-845.	4.8	7
125	The architecture of Tetrahymena telomerase holoenzyme. Nature, 2013, 496, 187-192.	13.7	99
126	The Smallest Capsid Protein Mediates Binding of the Essential Tegument Protein pp150 to Stabilize DNA-Containing Capsids in Human Cytomegalovirus. PLoS Pathogens, 2013, 9, e1003525.	2.1	46

#	Article	IF	CITATIONS
127	Single Particle Electron Microscopy Analysis of the Bovine Anion Exchanger 1 Reveals a Flexible Linker Connecting the Cytoplasmic and Membrane Domains. PLoS ONE, 2013, 8, e55408.	1.1	21
128	A new topology of the HK97-like fold revealed in Bordetella bacteriophage by cryoEM at 3.5 Ã resolution. ELife, 2013, 2, e01299.	2.8	49
129	Atomic Structure of Bordetella Bacteriophage Reveals a Jellyroll Fold in Cement Protein and a Topologically Distinct HK97-like Fold in Major Capsid Protein. Microscopy and Microanalysis, 2012, 18, 72-73.	0.2	2
130	Ultrastructural analysis of neuronal synapses using state-of-the-art nano-imaging techniques. Neuroscience Bulletin, 2012, 28, 321-332.	1.5	12
131	Seeing Engineered Loops in a Gene Delivery Vehicle by cryoEM. Structure, 2012, 20, 1286-1288.	1.6	2
132	Three-Dimensional Structure of the Trypanosome Flagellum Suggests that the Paraflagellar Rod Functions as a Biomechanical Spring. PLoS ONE, 2012, 7, e25700.	1.1	42
133	Biochemical and structural characterization of the capsid-bound tegument proteins of human cytomegalovirus. Journal of Structural Biology, 2011, 174, 451-460.	1.3	46
134	Limiting factors in atomic resolution cryo electron microscopy: No simple tricks. Journal of Structural Biology, 2011, 175, 253-263.	1.3	63
135	Atomic resolution cryo electron microscopy of macromolecular complexes. Advances in Protein Chemistry and Structural Biology, 2011, 82, 1-35.	1.0	70
136	Atomic Model of CPV Reveals the Mechanism Used by This Single-Shelled Virus to Economically Carry Out Functions Conserved in Multishelled Reoviruses. Structure, 2011, 19, 652-661.	1.6	61
137	Drug Delivery: Vaults Engineered for Hydrophobic Drug Delivery (Small 10/2011). Small, 2011, 7, 1431-1431.	5.2	0
138	Assembly of Vesicular Stomatitis Virus. , 2011, , 175-191.		1
139	Electron Tomography Reveals Polyhedrin Binding and Existence of both Empty and Full Cytoplasmic Polyhedrosis Virus Particles inside Infectious Polyhedra. Journal of Virology, 2011, 85, 6077-6081.	1.5	18
140	Hydrogen-bonding networks and RNA bases revealed by cryo electron microscopy suggest a triggering mechanism for calcium switches. Proceedings of the National Academy of Sciences of the United States of America, 2011, 108, 9637-9642.	3.3	111
141	Alanine 32 in PilA is important for PilA stability and type IV pili function in Myxococcus xanthus. Microbiology (United Kingdom), 2011, 157, 1920-1928.	0.7	13
142	Atomic Structure of Human Adenovirus by Cryo-EM Reveals Interactions Among Protein Networks. Science, 2010, 329, 1038-1043.	6.0	325
143	Correcting for the Ewald Sphere in High-Resolution Single-Particle Reconstructions. Methods in Enzymology, 2010, 482, 369-380.	0.4	24
144	Bluetongue virus coat protein VP2 contains sialic acid-binding domains, and VP5 resembles enveloped virus fusion proteins. Proceedings of the National Academy of Sciences of the United States of America, 2010, 107, 6292-6297.	3.3	97

#	Article	IF	CITATIONS
145	Low cost, high performance GPU computing solution for atomic resolution cryoEM single-particle reconstruction. Journal of Structural Biology, 2010, 172, 400-406.	1.3	23
146	Backbone Model of an Aquareovirus Virion by Cryo-Electron Microscopy and Bioinformatics. Journal of Molecular Biology, 2010, 397, 852-863.	2.0	85
147	3.3 Ã Cryo-EM Structure of a Nonenveloped Virus Reveals a Priming Mechanism for Cell Entry. Cell, 2010, 141, 472-482.	13.5	292
148	Cryo-EM Model of the Bullet-Shaped Vesicular Stomatitis Virus. Science, 2010, 327, 689-693.	6.0	205
149	Electron microscopy and threeâ€dimensional (3D) reconstruction of fullâ€length anion exchanger 1 (AE1). FASEB Journal, 2010, 24, 1002.1.	0.2	0
150	3.88 à structure of cytoplasmic polyhedrosis virus by cryo-electron microscopy. Nature, 2008, 453, 415-419.	13.7	257
151	Towards atomic resolution structural determination by single-particle cryo-electron microscopy. Current Opinion in Structural Biology, 2008, 18, 218-228.	2.6	163
152	Structures of the Human Pyruvate Dehydrogenase Complex Cores: A Highly Conserved Catalytic Center with Flexible N-Terminal Domains. Structure, 2008, 16, 104-114.	1.6	70
153	Symmetry-adapted spherical harmonics method for high-resolution 3D single-particle reconstructions. Journal of Structural Biology, 2008, 161, 64-73.	1.3	42
154	Subnanometer-Resolution Structures of the Grass Carp Reovirus Core and Virion. Journal of Molecular Biology, 2008, 382, 213-222.	2.0	118
155	Structure and Assembly of Human Herpesviruses: New Insights From Cryo-Electron Microscopy and Tomography. , 2008, , 483-516.		1
156	Direct Visualization of the Putative Portal in the Kaposi's Sarcoma-Associated Herpesvirus Capsid by Cryoelectron Tomography. Journal of Virology, 2007, 81, 3640-3644.	1.5	35
157	Dissecting human cytomegalovirus gene function and capsid maturation by ribozyme targeting and electron cryomicroscopy. Proceedings of the National Academy of Sciences of the United States of America, 2005, 102, 7103-7108.	3.3	33
158	Cytoplasmic Polyhedrosis Virus Structure at 8 Ã by Electron Cryomicroscopy. Structure, 2003, 11, 651-663.	1.6	64
159	Three-Dimensional Structures of the A, B, and CCapsids of Rhesus Monkey Rhadinovirus: Insights into GammaherpesvirusCapsid Assembly, Maturation, and DNAPackaging. Journal of Virology, 2003, 77, 13182-13193.	1.5	28
160	Structural Comparisons of Empty and Full Cytoplasmic Polyhedrosis Virus. Journal of Biological Chemistry, 2003, 278, 1094-1100.	1.6	35
161	Database Integration and the Web Portal Development for the IMIRS 3D Reconstruction Package. Microscopy and Microanalysis, 2003, 9, 964-965.	0.2	0
162	IMIRS: a high-resolution 3D reconstruction package integrated with a relational image database. Journal of Structural Biology, 2002, 137, 292-304.	1.3	87

#	Article	IF	CITATIONS
163	Molecular Interactions and Viral Stability Revealed by Structural Analyses of Chemically Treated Cypovirus Capsids. Virology, 2002, 298, 45-52.	1.1	10
164	Three-Dimensional Structure of the Human Herpesvirus 8 Capsid. Journal of Virology, 2000, 74, 9646-9654.	1.5	71
165	Visualization of Tegument-Capsid Interactions and DNA in Intact Herpes Simplex Virus Type 1 Virions. Journal of Virology, 1999, 73, 3210-3218.	1.5	229
166	On The Unique Structural Organization of the Saccharomyces Cerevisiae Pyruvate Dehydrogenase Complex. Microscopy and Microanalysis, 1998, 4, 954-955.	0.2	1
167	LETTER TO THE EDITOR: Confidence Interval Estimates of an Index of Quality Performance Based on Logistic Regression Models, by David W. Hosmer and Stanley Lemeshow,Statistics in Medicine,14, 2161-2172 (1995). Statistics in Medicine, 1997, 16, 1301-1303.	0.8	9
168	Changes in plasma warfarin levels and variations in steady-state prothrombin times. Clinical Pharmacology and Therapeutics, 1995, 58, 588-593.	2.3	25
169	Assembly of VP26 in herpes simplex virus-1 inferred from structures of wild-type and recombinant capsids. Nature Structural and Molecular Biology, 1995, 2, 1026-1030.	3.6	152